

Article

The Mechanism of Viscosity-Enhancing Admixture in Backfill Slurry and the Evolution of Its Rheological Properties

Liuhua Yang ^{1,*}, Hengwei Jia ¹, Huazhe Jiao ¹, Mengmeng Dong ² and Tongyi Yang ³

¹ School of Civil and Engineering, Henan Polytechnic University, Jiaozuo 454000, China; jhw912@126.com (H.J.); jiaohuazhe@hpu.edu.cn (H.J.)

² School of Materials, Henan Polytechnic University, Jiaozuo 454000, China; 15239593480@163.com

³ School of Environmental and Chemical Engineering, Jiangsu University of Science and Technology, Zhenjiang 212003, China; tongyi@just.edu.cn

* Correspondence: yanglh2005@163.com

Abstract: Since filling slurry is a cement-based material, viscosity-enhancing admixture exerts a significant effect on its rheological performance and mechanical properties. Viscosity-enhancing admixture can improve pipeline transportation performance and reduce pipeline wear during the filling process of a kilometer-deep mine by changing the plastic viscosity and yield stress of high-concentration filling slurries. In order to reveal the influence mechanism of viscosity-enhancing admixture on rheological performance in slurry, the influence of viscosity-enhancing admixture on the rheological performance of slurry is explored by adjusting viscosity-enhancing admixture dosage and conducting bleeding test, liquidity test, and rheological performance test. The extended DLVO theory is employed to analyze the mechanism of HPMC on the stability of filling slurry. The results show that compared with ordinary slurry, after adding HPMC and XG, the particles of filling slurry are prone to link to form a mesh structure. Besides, the increasing frictional force between particles results in a significant decrease in the bleeding rate and liquidity of the slurry. Such an effect becomes more obvious with the increase of viscosity-enhancing admixture dosage. Meanwhile, the overall effect of HPMC molecules is better than that of XG molecules since HPMC can reduce inter-particle repulsion and facilitate particle aggregation. The optimal dosage is about 0.1%, at which time the yield stress of the filling slurry increases from 89.236 to 160.06 Pa, the plastic viscosity increases from 0.296 to 1.063 Pa·s, and the compressive strength increases from 2.58 to 3.59 MPa in 28 days. The study reveals the influence of viscosity-enhancing admixture on the rheological performance of filling slurry and its evolution characteristics, which provides theoretical support for the development of filling resistance and wear reduction technology.

Keywords: paste slurry; hydroxypropyl methylcellulose (HPMC); xanthan gum (XG); bleeding rate; rheological performance



Citation: Yang, L.; Jia, H.; Jiao, H.; Dong, M.; Yang, T. The Mechanism of Viscosity-Enhancing Admixture in Backfill Slurry and the Evolution of Its Rheological Properties. *Minerals* **2023**, *13*, 1045. <https://doi.org/10.3390/min13081045>

Academic Editor: Abbas Taheri

Received: 29 June 2023

Revised: 2 August 2023

Accepted: 4 August 2023

Published: 6 August 2023



Copyright: © 2023 by the authors. Licensee MDPI, Basel, Switzerland. This article is an open access article distributed under the terms and conditions of the Creative Commons Attribution (CC BY) license (<https://creativecommons.org/licenses/by/4.0/>).

1. Introduction

Mining and utilizing mineral resources stimulate economic growth and generate substantial sediments and goaf [1–3]. China's total stockpile of tailings exceeds 25 billion tons, which wastes land resources and poses grave safety risks. Not only does this deplete land resources, but it also increases security hazards. Due to its environmental and economic benefits, backfill mining has become an excellent choice for resolving mining development issues in light of the pressing need for resource development. Presently, paste infill is extensively used in both coal and non-coal mines. Utilizing tailings for paste filling can reduce the quantity of waste and increase the rate of mineral resource recovery. Therefore, paste filling technology has become the leading direction for the development of filling mining [4,5].

Due to its high conveying efficiency, high-flow paste slurry has become the preferred form of paste filling as a result of the development and innovation of paste-filling

technology [6–8]. Components, including cementitious materials, aggregates, water, and admixtures, will affect the efficacy of the paste slurry [9–12]. Due to poor stability, high-viscosity paste slurry is susceptible to segregation and leakage, negatively impacting the paste's workability, strength, and durability [13]. Nevertheless, the thickener can ensure the cohesion of the slurry during the filling process while also accelerating the construction process [14]. Therefore, in engineering practice, the thickener is used as a substance that changes the viscosity of the paste. Over the years, various types of thickeners have been added to paste slurries, including organic thickeners, such as cellulosic thickeners, polysaccharide thickeners, and polypropylene thickeners, as well as inorganic thickeners (inorganic salt thickeners and inorganic gel thickeners) [15,16]. Cellulosic thickeners are extensively employed in paste filling applications due to their low dosage requirements and excellent performance. The hydration and mechanical properties of this material have been extensively researched and analyzed by numerous domestic and international scholars. The study demonstrates that the thickener has the ability to modify the slurry's yield stress and plastic viscosity, enhance the stability of the paste, and mitigate issues related to segregation and leakage. According to research, hydroxypropyl methylcellulose (HPMC), warm-mixed rubber, and polyacrylic thickeners [17,18] can all reduce the extensibility and slump of concrete while increasing its water retention. Patural [19] investigated how cellulose affected the rheological and water retention characteristics of mortar. The outcomes demonstrated that, at a dose of 0.27 wt%, cellulose showed a substantial thickening impact and water retention performance, with the capacity for water retention increasing with increasing molecular weight. Zhang et al. [20] investigated the effect of Wenlun rubber on the functionality of a slurry with a high water-cement ratio. The outcomes demonstrate that the warm-mixed rubber slurry has outstanding thickening performance, can address bleeding and segregation issues, and can enhance slurry water retention performance. The water retention mechanism of hydroxyethyl cellulose (MHEC) was researched by Bulichen et al. [21], who discovered that at low dosages, MHEC achieves water retention performance by absorbing water molecules. In contrast, HEMC produces network gel at large dosages by drinking water and swelling. The structure prevents free water from moving freely by obstructing the slurry's pores [22,23]. The research mentioned above provides a thorough explanation of the technical benefits and viability of thickeners in the field of high-concentration paste filling. These analyses, however, have been carried out at the surface or in shallow filling situations [24–27], and more consideration needs to be given to construction circumstances that call for delving thousands of meters below ground.

Based on findings from prior studies, this study analyses how thickeners affect the flow and rheological characteristics of paste slurry. The experiment contrasted the frequently used thickening ingredient hydroxypropyl methylcellulose (HPMC) [28] with the less studied but environmentally friendly and renewable xanthan gum (XG) [29]. The impact of thickeners on the bleeding, fluidity, and rheological characteristics of paste slurry was studied by varying the number of thickeners (HPMC and XG). The DLVO theory was introduced to describe the characteristics of particle evolution quantitatively, and the mechanical performance test of the paste was conducted to elucidate the mechanism of HPMC and XG on the flow and rheological properties of the paste slurry.

2. Materials and Methods

2.1. Materials

The experimental material consists of Shandong mining facility tailings. Figure 1 depicts the particle size distribution curve acquired after measuring tailings with a laser particle size analyzer (LMS-30). The volume fraction of particles less than 20 μm in the tailings is 37.3%, which satisfies the minimum requirements for producing a paste. The average particle size of tailings is computed to be 76.2 μm , while the curvature coefficient [30] is 0.85 and the inhomogeneity coefficient is 14.72. An inhomogeneity coefficient greater than 5 for granular materials denotes a broad particle distribution range and excellent gradation. A curvature coefficient between 1 and 3 represents a more compact structure. In

conclusion, the tailings have a broad particle size distribution and excellent gradation but poor compaction. The XRF measurements of the sediments are presented in Table 1.

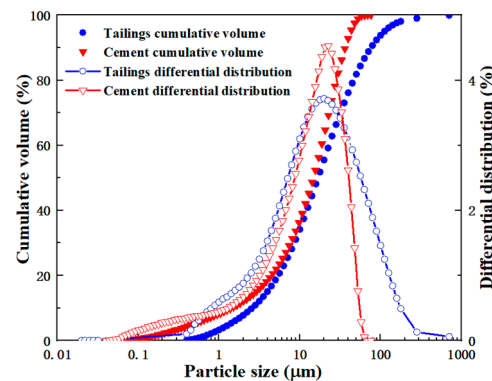


Figure 1. Particle size distribution of tailings.

Table 1. Main chemical composition of tailings.

Components	Pb	Zn	S	As	Cu	Ag	CaO	MgO	Al ₂ O ₃	SiO ₂
Concentration (%)	0.7	0.03	0.39	0.057	0.05	1.59	9.26	1.4	6.19	64.68

Figure 1 depicts the particle size distribution of the cementitious material, which is 42.5R ordinary silicate cement with an average particle size of 37 μm . According to XRF detection, the specific surface area is $401 \text{ m}^2 \cdot \text{kg}^{-1}$, the specific gravity is 3.15, and Table 2 displays its chemical composition. Deionized water was used to prepare the experimental samples to eliminate interference from impurities in the water on the experimental results.

Table 2. Main chemical components of cement.

Compound	MgO	SiO ₂	Na ₂ O	K ₂ O	Al ₂ O ₃	SO ₃	Fe ₂ O ₃	CaO	Others
Content (%)	1.40	20.70	0.18	0.48	4.50	2.60	3.30	65.10	1.74

Select polysaccharides xanthan gum (XG) and cellulose hydroxypropyl methylcellulose (HPMC) for orthogonal experiments and choose the admixture with the best effect and the most significant economic applicability.

2.2. Experimental Program

In the beginning, add the tailings and cementitious materials to a 3 L container and stir by hand for one minute. Then, add the thickener to the specified amount of deionized water and stir until it is fully dissolved. Next, pour the solution into a bucket and stir it by hand for 1 min to acquire a relatively homogenous mixture. Then, mix the paste at 125 rpm for 5 min until it is homogenous. Transfer the substance sample immediately into the laboratory beaker and initiate the rheological experiment with the Brookfield R/S paddle rheometer. Table 3 lists the slurry ratios, with a total of 11 experimental groups established. Among them, there are two different thickeners and five typical dosages.

All sample preparation procedures, proportions, and ambient temperatures were kept constant to reduce other factors' influence on the experimental results. Then, each experimental group used a constant sand-to-cement ratio (1:8) to produce a 72% mass concentration slurry. Based on the ratio, the respective amounts of thickener in the slurry were 0, 0.42, 0.84, 1.27, 1.69, and 2.11 g. The thickener solution is mixed directly with the slurry, and the product preparation takes 300 s.

Table 3. Experimental samples ratio.

Group	Dosage (%)	Tailings (g)	Cement (g)	Water (g)	
N-1	— —	0.000%	1500	187.5	583.3
XG-2	XG	0.025%	1500	187.5	583.3
XG-3		0.050%	1500	187.5	583.3
XG-4		0.075%	1500	187.5	583.3
XG-5		0.100%	1500	187.5	583.3
XG-6		0.125%	1500	187.5	583.3
HP-2		HPMC	0.025%	1500	187.5
HP-3	0.050%		1500	187.5	583.3
HP-4	0.075%		1500	187.5	583.3
HP-5	0.100%		1500	187.5	583.3
HP-6	0.125%		1500	187.5	583.3

2.3. Test Methods

2.3.1. Bleeding Test

The quantity of slurry bleeding is measured using a 1000 mL standard experimental measuring cylinder that has been dried. First, divide the thoroughly mixed slurry into the measuring instrument twice, approximately 500 mL each time. Then, densify from edge to center until there are no more voids. Next, wipe the surface and entrance of the measuring cylinder, and then begin timing. Measurement time is 15, 30, 45, 60, 90, and 120 min. Lastly, suction the blood into a 10 mL graduated cylinder using a rubber dropper and document the volume.

2.3.2. Mobility Test

The flow measurement uses the “Cement Mortar Fluidity Test Method”. The experimental slurry will be poured into the mold, and the upper surface will be leveled. The mold must be removed slowly to eradicate other potential influences from the experiment. The instrument uses a slump cone (XN-50 × 100 × 150 mm).

2.3.3. Rheology Test

The equipment used in the investigation is an R/S rheometer by Brookfield. Maintain an indoor temperature of 20 °C ± 1 °C to minimize experimental errors. The rotor (VT-40-20) has a diameter of 20 mm and a height of 40 mm to prevent the wall slip effect and harm to the slurry structure during entry. The rheological test was conducted by regulating the shear rate, which was increased from 0 s⁻¹ to 150 s⁻¹ throughout 150 s. The sample is not sheared beforehand to prevent material flow and other factors from influencing the experimental results.

2.3.4. Strength Test

The paste slurry is prepared according to the planned ratio and poured into standard test molds (70.7 × 70.7 × 70.7 mm) for maintenance. All testing procedures are conducted under ASTM-C1437. Each strength value is the average value derived from more than five uniaxial compressive strength (UCS) tests. UCS tests were undertaken after curing for predetermined periods (3, 7, and 28 days). The mechanical properties were examined using a 50 kN-loading press. The press’s displacement speed was regulated at 0.5 mm/min during the experiment.

3. Results

3.1. Bleeding Characteristics

This experiment aims to determine whether the action of the thickener impacts the slurry’s ability to retain water. Figure 2 depicts the bleeding rate of the paste slurry at various HPMC and XG concentrations. With increasing amounts of HPMC and XG, the

bleeding rate of the paste slurry is reduced, and the bleeding situation is improved, but the degree of reduction varies significantly. At 120 min, the slurry attained a maximum bleeding rate of 12.8% without adding a thickener. When HPMC is added and the dosage is increased from 0.025% to 0.125%, the bleeding rate of the slurry for 120 min is reduced from 12.8% to 2.5%, and there is almost no overflowing water on the surface of the slurry. However, when XG was added and the dosage increased from 0.025% to 0.125%, the bleeding rate of the slurry at 120 min decreased from 12.8% to 7.2%. Comparatively, at the exact dosage, the water retention rate of HPMC is generally about 5% higher than that of XG, indicating that the water retention efficiency of HPMC is significantly greater than that of XG.

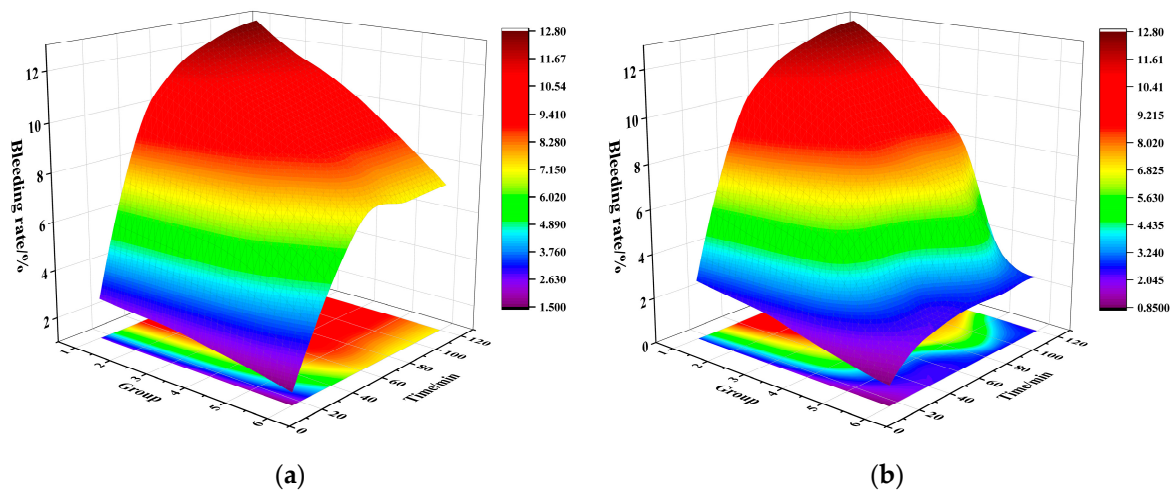


Figure 2. Bleeding rate under different thickeners: (a) XG, (b) HPMC.

The primary reason for this is that the molecular structure of HPMC contains hydroxyl(-OH) and ether bonds(-O-), and the water molecules combine with the oxygen atoms on the groups to form hydrogen bonds, thereby binding the free water molecules. HPMC molecules are adsorbed to the surface of mineral particles to increase their water-retention capacity. In addition to carboxyl groups, XG possesses a certain degree of cross-linking. Through hydration of the hydrophilic portion and cooperation with electrostatic repulsion between polymer molecules, the coil structure of the polymer is wholly unwound to accomplish the water retention effect. In contrast, HPMC can link particles to form a more stable network structure, allowing free water to be fixed within the system and restricting the free movement of water molecules, thereby preventing water loss in the slurry.

3.2. Flow Characteristics

The thickener can effectively reduce the fluidity of the paste slurry, aggregate the paste slurry's particles, and improve the paste slurry's anti-bleeding and segregation properties. The small-scale slump flow test is suitable for assessing the flow characteristics of paste slurries containing additives. Figure 3 and Table 4 show the outcomes of tests on the flow characteristics of thickeners.

The deformability Γ is given by

$$\Gamma = (d^2 - d_0^2) / d_0^2 \quad (1)$$

where Γ is the deformability, d_0 is the diameter of small-scale slump cone, d is the fluidity of paste.

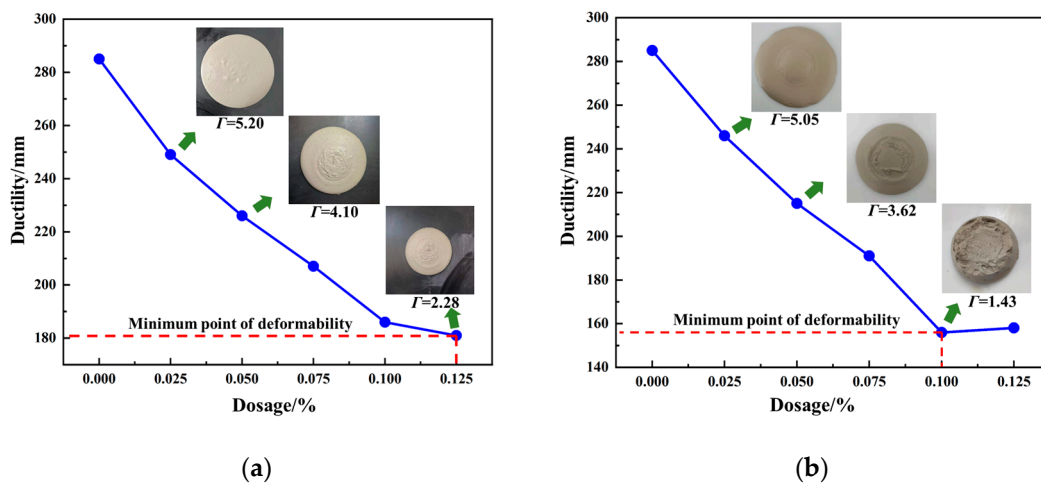


Figure 3. Influence of thickener dosing on slurry ductility: (a) XG, (b) HPMC.

Table 4. Results of Γ of paste slurry.

Group	d_0 (mm)	d (mm)	Γ
N-1	100	285	7.12
XG-2	100	249	5.20
XG-3	100	226	4.10
XG-4	100	207	3.28
XG-5	100	186	2.46
XG-6	100	181	2.28
HP-2	100	246	5.05
HP-3	100	215	3.62
HP-4	100	191	2.65
HP-5	100	156	1.43
HP-6	100	158	1.49

As shown in Figure 3, both HPMC and XG can effectively reduce cement paste's fluidity as the dosage increases, and the paste slurry's fluidity will decrease. HPMC connects the particles to form a flocculation structure, which is the primary cause. When the flocculation structure increases, so does the friction between the slurry particles, the fluidity of the slurry decreases, and the cement slurry becomes more viscous. Moreover, the molecules of HPMC and XG have ether bonds and hydroxyl groups, which can combine with water molecules in the paste slurry to reduce the dispersion of the cement slurry, thicken the paste slurry, and make it less fluid. Table 4 demonstrates that HPMC has a more significant effect on the fluidity of paste slurry at the exact dosage. When the concentrations of HPMC and XG are less than 0.05%, the disparity between their effects on the deformation ability of the paste slurry is minimal. When the addition amount exceeds 0.075%, the slump of the HPMC group decreases from 191 to 156 mm, the deformability of the slurry decreases from 2.65 to 1.43, the recession of the XG group decreases from 207 to 181 mm, and the deformability of the slurry ability decreases from 3.28 to 2.28. The effect of XG was 9% less than that of HPMC. In addition, after the quantity of HPMC reaches 0.1%, the fluidity of the paste slurry decreases to below 160 mm, and there is no discernible change as the amount increases. Inferences suggest that the optimal concentration of HPMC is approximately 0.1%. Under identical dosage conditions, HPMC can reduce the flowability of the paste slurry more than XG, indicating that HPMC has a more significant effect on lowering the flowability of the paste slurry than XG.

3.3. Rheological Performance

The paste slurry was subjected to rheological tests to determine the effect of thickeners on its rheological properties. The effects of two types of thickeners on the shear stress and apparent viscosity of paste slurry are illustrated in Figures 4 and 5. In contrast, the effects on yield stress and plastic viscosity are depicted in Table 5.

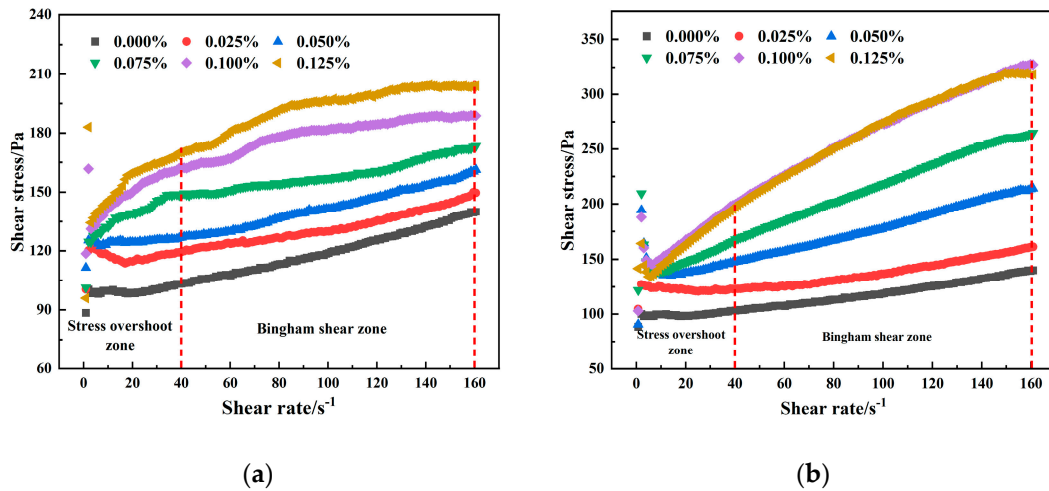


Figure 4. Relationship between paste shear stress and shear rate under various schemes: (a) XG, (b) HPMC.

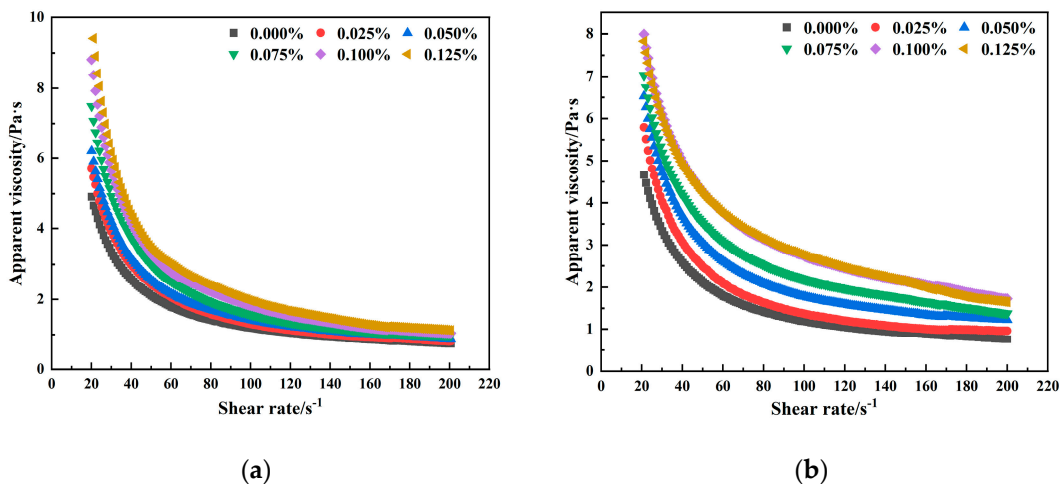


Figure 5. Relationship between apparent viscosity and shear rate under various schemes: (a) XG, (b) HPMC.

As shown in Figure 4, the shear stress of the slurry increases as the shear rate increases. At a constant shear rate, the greater the thickener, the higher the shear stress because the more influential the thickener, the more entangled the aggregates, and the greater the external force required to make the slurry produce deformation. HPMC lets the slurry have a higher shear stress than XG, mainly because HPMC significantly affects particle entanglement and adhesion, has a larger particle aggregate size, is more robust in intermolecular entanglement, and has a stronger hinge structure. The external force necessary to effect the exact change increases at low shear rates. Under the condition of the exact dosage and the same shear rate, HPMC is the one that increases the shear stress the most, followed by XG.

Table 5. Fitting results of experimental data based on Bingham plasticity model.

Group	Yield Stress (Pa)	Plastic Viscosity (Pa·s)	R ²
N-1	89.236	0.296	0.992
XG-2	108.991	0.311	0.971
XG-3	113.832	0.334	0.994
XG-4	138.583	0.389	0.968
XG-5	156.349	0.542	0.966
XG-6	164.714	0.633	0.964
HP-2	106.097	0.324	0.991
HP-3	122.311	0.572	0.993
HP-4	134.455	0.838	0.998
HP-5	160.064	1.063	0.996
HP-6	164.655	1.051	0.983

The apparent viscosity of a paste slurry is one of the key indicators used to assess its rheological performance. Figure 5 demonstrates that the apparent viscosities of the blank group and the paste slurry containing a thickener decrease as the shear rate increases, indicating the existence of shear thinning. The particles in the paste slurry are interconnected to form larger aggregates, and the molecules of the thickening agent adhere to the surface of the particles, enhancing their ability to interconnect. When the shear rate is low, it cannot provide enormous stress to open the aggregates, so the maximum apparent viscosity occurs at low shear rates. As the shear rate increases, entangled particles transition from disorder to order, shear stress gradually increases, particle aggregates within the paste slurry are gradually opened, and apparent viscosity gradually decreases. When the dosage of thickener and shear rate are identical, the paste slurry containing HPMC has the highest apparent viscosity, followed by XG.

In order to measure the functional performance of paste slurry more accurately, the Herschel–Bulkley model [31] can be used to characterize the paste's rheological parameters. The expression model is:

$$\tau = \tau_0 + \mu_\beta \left(\frac{d_v}{d_h} \right)^\lambda \quad (2)$$

In the equation, where τ is the shear stress, τ_0 is the dynamic yield stress, μ_β is the plastic viscosity, d_v/d_h is the shear rate, and λ is the index of flow performance.

When $\lambda < 1$, the rheology of the paste conforms to the yielding pseudoplastic model. When $\lambda > 1$, the rheology of the paste conforms to the yielding dilatant model. When $\lambda = 1$, the rheology of the paste conforms to the Bingham plastic model. Figure 4 displays the rheological data for each experimental plan, which are separated into the Bingham shear zone ($0\sim 40 \text{ s}^{-1}$) and the stress overshoot influence zone ($40\sim 160 \text{ s}^{-1}$) based on the characteristics of yield stress change. As shown in Table 4, fit the Bingham shear zone data. The rheological constitutive model of the paste is consistent with the Bingham plastic body model, as shown by the goodness-of-fit coefficients, which are all greater than 0.96 ($R^2 > 0.96$).

The paste slurry's plastic viscosity and yield stress rise when HPMC and XG concentration increases, as indicated in Table 4, consistent with the fluidity variation trend. When the HPMC dosage is 0.10%, the plastic viscosity is 1.063 Pa·s, and the yield stress is 160.604 Pa. Continuing to increase the dosage of HPMC did not result in improvement, indicating that the optimal dosage of HPMC is 0.10%. At this dosage, the water retention effect is significantly improved. The plastic viscosity is 0.542 Pa·s, and the yield stress is 156 Pa when the XG dosage is 0.10%. The viscosity at the same yield stress is 51% of the HPMC value, demonstrating that XG has a less significant impact than HPMC.

The DLVO theory [32] is introduced to measure the impact of HPMC dosage on the slurry's yield stress. The impact of the thickener on the paste slurry's ability to flocculate was calculated using the force between particle interactions. Calculating the van der Waals

force is necessary to analyze how the polymer thickener affects the mutual attraction between particles in the paste slurry. The formation of the flocculation structure in paste slurry is primarily influenced by the van der Waals force, which includes the dispersion force, opposing force, and induced coupling force. When calculating the force of interaction between two particles, two spheres of equal volume can be used as a model. When the distance between the two spheres is h which is much smaller than the particle radius R , the formulas for calculating the van der Waals gravitational potential energy between two spherical particles are shown in Formulas (3) and (4).

$$F_V = \frac{RA}{12h^2} \quad (3)$$

$$V_V = -\frac{HA}{12h} \quad (4)$$

As the equation shows, where A is the Hamaker constant of paste and thickener in water, J ; R is the average radius of particles, taken as 76.2×10^{-6} m; h is the distance between two particles, m.

The H in Formula (3) is the Hamaker effective constant, which is determined by the type of particles and the type of medium in which the particles are located. Water is about 3.7×10^{-20} J, cement is about 9.6×10^{-20} J, and HPMC is about 14.9×10^{-20} J. We combine the constants of the individual particles, and the medium yields the dispersion of Hamaker's constant A_{132} (see Equation (5)).

$$A_{132} = \left(\sqrt{A_1 - A_3}\right) \left(\sqrt{A_2 - A_3}\right) \quad (5)$$

In the equation, where A_{132} is the effective Hamaker constant of cement and HPMC in aqueous medium, A_1 is the Hamaker constant of the particles, A_2 is the Hamaker constant of HPMC, and A_3 is the Hamaker constant of water.

According to the DLVO theory, van der Waals attraction and electrostatic repulsion are the main forces acting on colloidal particles. The potential energy of electrostatic repulsion is shown in (6). The particle surface will absorb ions from the paste slurry as the paste hydrates. As a result, a diffusion layer and an adsorption layer will form on the particle surface, creating an electrostatic force between nearby particles.

$$V_E = 2\pi\epsilon_0\epsilon_\gamma R\psi_{dl}^2 e^{-kh} \quad (6)$$

where ϵ_0 is the permittivity of vacuum, $\epsilon_0 = 8.854 \times 10^{-12}$ C/(V·m); ϵ_γ is the dielectric constant of water, $\epsilon_\gamma = 78.36$ F/m; ψ_{dl} is the electric potential of the diffuse layer, V; and the screening parameter κ is given by

$$\kappa^2 = \frac{4e^2 N_A I}{\epsilon_0 \epsilon_\gamma K_B T} \quad (7)$$

where N_A is the Avogadro's number, 6.022×10^{23} /mol; K_B the Boltzmann constant, 1.380649×10^{-23} J/K; T the absolute temperature, 298.15 K; e is the elementary charge, 1.6×10^{-19} C; and I is the ionic strength, mol/L. The latter quantity is defined by

$$I = \frac{1}{2} \sum_{i=1}^n c_i z_i^2 \quad (8)$$

whereby the electrolyte solution contains ions of type i with valence z_i and molar concentration c_i .

Assuming that the particles in the paste slurry are spherical colloidal particles, the total potential energy between particles is the sum of the van der Waals gravitational and repulsive potential energy. The total potential energy is represented by Formula (9).

$$V_{Total} = V_V + V_E \quad (9)$$

where V_{Total} is the Total inter-particle potential energy, $K_B T$; V_V is the inter-particle van der Waals gravitational potential energy, $K_B T$; V_E is the inter-particle electrostatic repulsion, $K_B T$.

To this end, the influence of different dosages of HPMC on the potential energy of attraction and repulsion between particles is drawn into a curve, and the influence curve shown in Figure 6 is obtained. Figure 6 shows that the repulsion barrier of the paste slurry mixed with HPMC is lower than that of the blank group. It can be seen from this that HPMC can improve the flocculation and sedimentation of the paste slurry.

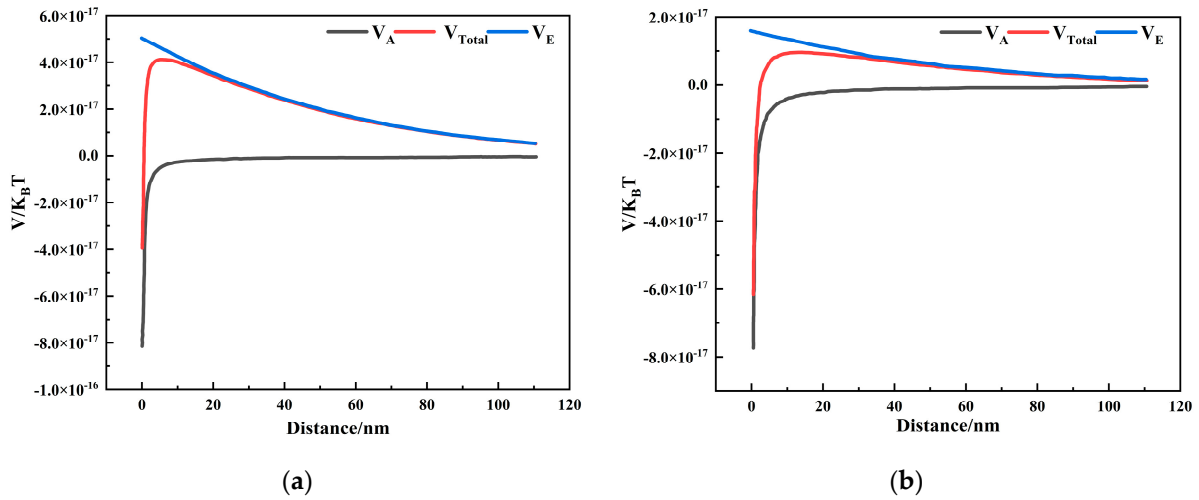


Figure 6. Effect of different dosages of HPMC on total potential energy between cement particles: (a) 0%, (b) 0.1% HPMC.

3.4. Detailed Analysis

During the hydration of the paste slurry, particles aggregate to form aggregates, which then connect to form a network-like flocculated structure. The internal aggregates in the slurry were observed to examine the correlation between the flowability and rheological properties of aggregates and paste slurries. A super depth of field is used to observe the aggregates within the paste slurry with 0%, 0.05%, 0.075%, and 0.1% thickener. Observation pictures of the aggregates within the paste slurry are depicted in Figure 7.

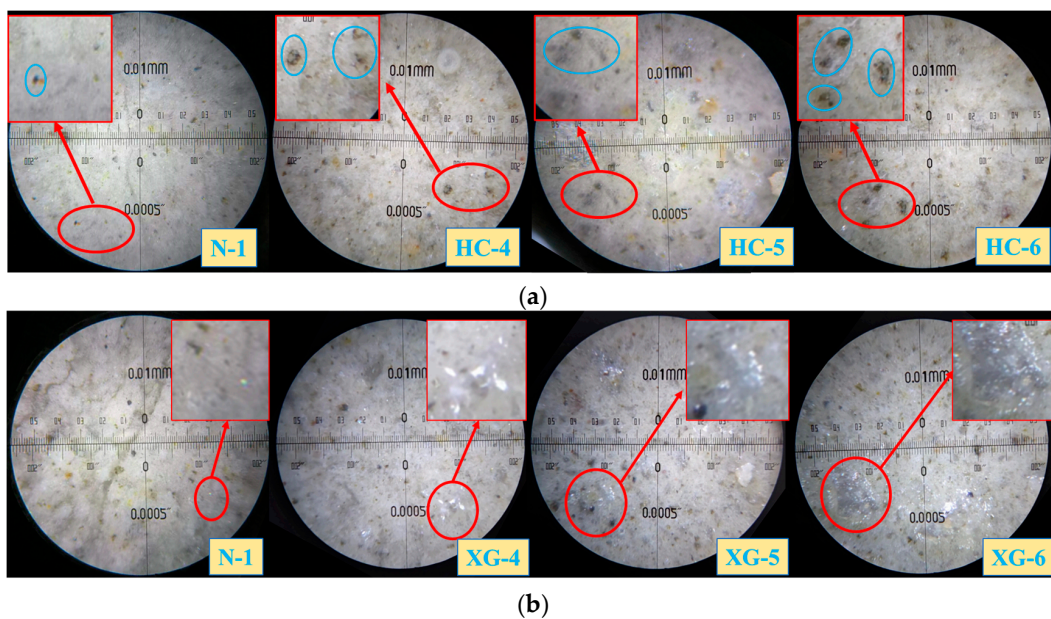


Figure 7. Influence of different polymer viscosity-enhanced agents on flocculation particles in cement paste: (a) Aggregation of particles, (b) growth in bubbles.

A super depth of field is used to observe the aggregates within the paste slurry with 0%, 0.05%, 0.075%, and 0.1% thickener. As the dosage of polymer thickener is increased, aggregate size progressively increases. When the dosage of HPMC is 0.1%, the aggregates in the slurry are the most significant, and their dispersion is the strongest. The network flocculation structure formed by the aggregation becomes more deformation-resistant as aggregate size increases. When the anti-deformation capability of the flocculation structure in the paste slurry is enhanced, its fluidity decreases, and its yield stress and plastic viscosity rheological parameters increase. However, by observing Figure 7b, it is found that with the increase of XG content, the number of micro-bubbles mixed with the whole tailings particles increases significantly during the hydration process. Air bubbles and water serve as lubricants, which is one of the reasons why the fluidity of XG slurry at the exact dosage is greater than that of HPMC slurry.

In Figure 7, through observing the images of the HP-5 and HP-6 groups, it's found that small particles begin to form aggregates, which are distributed relatively evenly in the paste slurry. However, in the XG-5 and XG-6 groups, as the number of small bubbles in the paste slurry increases significantly, these small bubbles are relatively concentrated together. In order to probe into the effect of these phenomena on the paste slurry's performance, some curing test specimens were split, and the cross-section was studied and analyzed. The results are shown in Figure 8. First, in the blank group, an effective mesh structure cannot form due to the repulsion between particles. Larger particles and aggregates sink rapidly, while smaller particles remain suspended, resulting in uneven settlement of the test specimens. Secondly, in the HP-4 group, the larger size of aggregates makes it easier to form a connected mesh structure, and the distribution of particles is more uniform and denser. Finally, in the XG-4 group, more small-scale bubbles in the paste slurry cause a large number of uneven pores inside the test specimens, which may have an effect on the compressive strength of the test specimens.

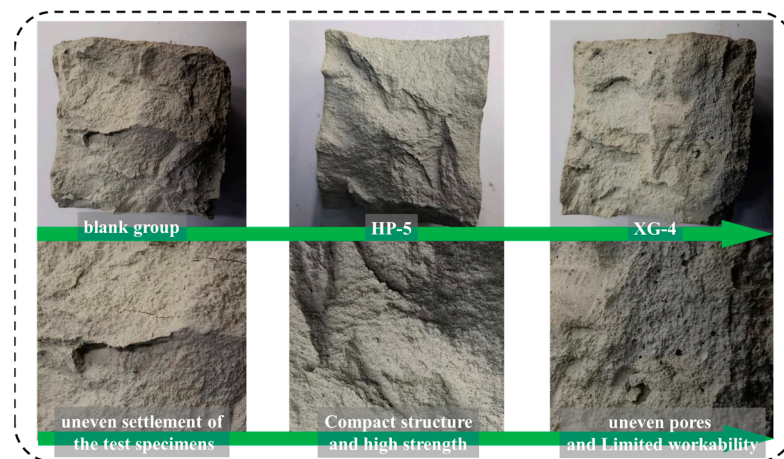


Figure 8. Sectional view of curing test specimens.

Based on the research findings, a schematic diagram of the evolution process of particle distribution with the addition of HPMC is proposed, as shown in Figure 9. HPMC molecules have a multi-segment structure. After HPMC is adsorbed on the surface of the particles, the segments on the HPMC molecules will rotate, aggregating the particles to form larger flocs, which are connected in the paste slurry. A flocculation structure resembling a net is formed.

3.5. Compressive Strength

Experiments were conducted on the mechanical properties of paste test blocks to verify the effect of thickeners. Figure 10 depicts the influence curve of different HPMC dosages on the compressive strength of the paste slurry at 3d, 7d, and 28d.

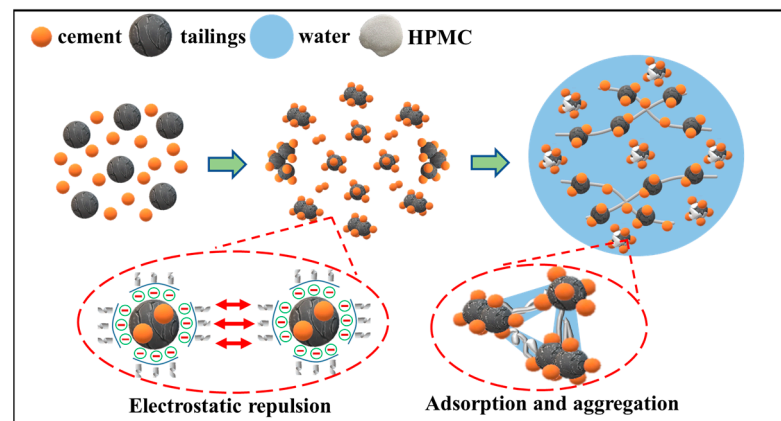


Figure 9. Action mechanism of thickener.

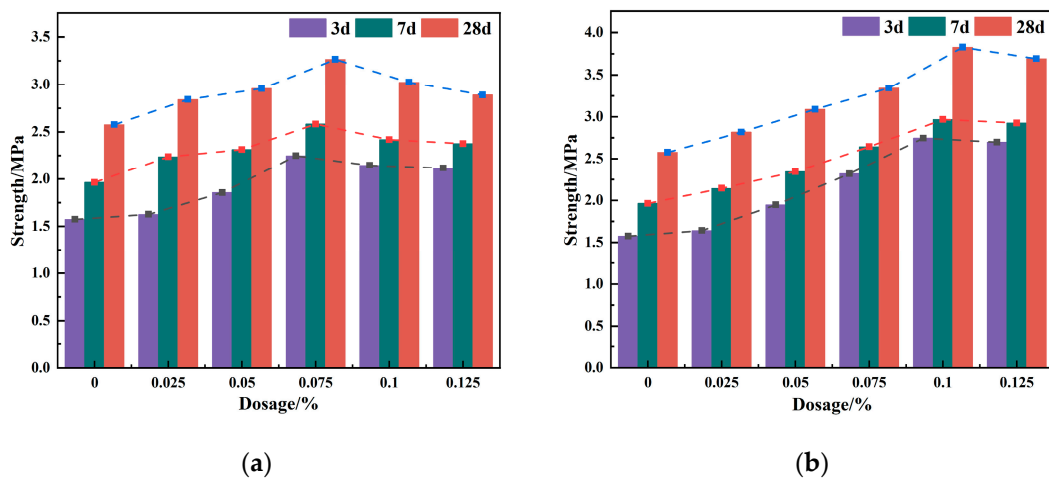


Figure 10. Influence of different polymer viscosity-enhanced agents on compressive strength: (a) XG, (b) HPMC.

Figure 10a illustrates the effect of varying xanthan gum dosages on the mechanical properties of the paste slurry. With the increase of XG content, the compressive strength of the paste test block showed an unstable increase. When the concentration of XG increased from 0% to 0.075%, the compressive strength increased by 26.7%. However, when the concentration of XG increased from 0.075% to 0.125%, the compressive strength decreased by 11.5%. This phenomenon may be due to the air-entraining effect of XG. As the dosage increases, so do the bubbles produced during the stirring process. The formed bubbles are surrounded by mineral particles and hydration products, making them difficult to expel from the hardened body. The formation of holes results in a weakened structure and altered mechanical properties (as shown in Figure 8).

Figure 10b demonstrates that the compressive strength of the paste test block increases significantly with increasing HPMC content. This phenomenon may be caused by the addition of HPMC to the paste slurry, which significantly improves the uneven distribution of particles and prevents the deposition of large particles at the bottom. Simultaneously, the rate of cement hydration reaction is slowed, and the resulting hydration product has a more uniform and compact structure. HPMC can enhance the test block's strength within the appropriate dosage range. Due to the small amount of HPMC added, the impact of HPMC molecules on the particles is not readily apparent at 0.025%. The paste test block's compressive strength at 7d and 28d is 2.14 and 2.72 MPa, respectively, an increase of approximately 8%. When the amount of thickener is increased to 0.1%, however, the compressive strength of paste test blocks 7d and 28d increases by approximately 37%. Increasing the amount of thickener does not significantly alter the mechanical properties

of the filling body when the amount of HPMC exceeds 0.1%, which is consistent with its effect on the rheology of the slurry.

In summary, the particle evolution within the paste is regulated by the viscosity-enhancing admixture (HPMC and XG). During deep filling, the shock vibrations of the slurry are amplified. This means that the slurry will be disturbed by external shear, which breaks the original relatively stable floc structure, and the relatively large particles lose the suspension of fine particles, and the slurry is prone to segregation, thus causing pipe plugging accidents. Nevertheless, thickeners can influence the yield stress and plastic viscosity of slurries by changing the particle distribution. The use of appropriate thickeners can ensure that the slurry remains cohesive during the filling process, improve the stability of the paste, and reduce problems associated with segregation and leakage. The research findings mentioned are of great significance for regulating the deep filling of paste.

4. Conclusions

- (1) The thickener influences the bleeding, fluidity, and yield stress by altering the paste slurry's free water and particle distribution. Bleeding and yield stress of slurry correlate positively with thickener concentration, whereas fluidity correlates negatively. Thickener can improve water retention by 5% to 10%, yield stress by 84%, and fluidity by 36.5% to 44.5%;
- (2) The thickener increases the paste slurry's compressive strength by improving the uneven settlement of the particles, thereby increasing the paste slurry's density. Within a specific dosage range, HPMC increases the compressive strength of the slurry, while XG harms the compressive strength of the slurry. When the concentration exceeds 0.075%, air bubbles will likely remain in the test block, resulting in a slight decrease in strength.
- (3) The optimal dosage of HPMC is 0.1%, with its effect being superior to that of XG. On the particle surface, HPMC molecules adsorb multiple fine-grained tailings to bridge and reduce the repulsion barrier between particles. Particles are easier to aggregate, strengthening the filling slurry's internal floc network structure, enhancing its structural stability, and increasing its resistance to gravity and external forces.

Author Contributions: Conceptualization, L.Y. and H.J. (Hengwei Jia); methodology, L.Y.; software, L.Y.; validation, H.J. (Hengwei Jia) and H.J. (Huazhe Jiao); formal analysis, H.J. (Huazhe Jiao); investigation, M.D.; resources, M.D.; writing—original draft preparation, T.Y.; writing—review and editing, L.Y.; visualization, H.J. (Huazhe Jiao); supervision, M.D.; project administration, L.Y.; funding acquisition, H.J. (Hengwei Jia). All authors have read and agreed to the published version of the manuscript.

Funding: This study was financially supported by the National Natural Science Foundation Project of China (No. 52104129), the Shandong Provincial Major Science and Technology Innovation Project, China (2019SDZY05), the key Laboratory of Mine Ecological Effects and Systematic Restoration, Ministry of Natural Resources (MEER-2022-09), the Double First-class Construction Project in Henan Province, China (AQ20230735), and the Doctoral Fund of Henan Polytechnic University (B2021-59).

Data Availability Statement: The data presented in this study are available on request from the corresponding author.

Conflicts of Interest: The authors declare no conflict of interest.

References

1. Jiao, H.Z.; Zhang, W.X.; Yang, Y.X.; Chen, X.M.; Yang, L.H. Static mechanical characteristics and meso-damage evolution characteristics of layered backfill under the condition of inclined interface. *Constr. Build. Mater.* **2023**, *366*, 130113. [[CrossRef](#)]
2. Jiao, H.Z.; Yang, W.B.; Zhen, R.; Yu, J.X.; Liu, J.H. The micro-scale mechanism of tailings thickening processing from metal mines. *Int. J. Miner. Metall. Mater.* **2022**, *68*, 21–31.
3. Wang, X.M.; Zhao, B.; Zhang, Q.L.; Xu, D.S. Cemented backfilling technology with unclassified tailings based on vertical sand silo. *J. Cent. South Univ. Technol.* **2008**, *15*, 801–807. [[CrossRef](#)]

4. Fall, M.; Célestin, J.; Sen, H. Potential use of densified polymer-pastefill mixture as waste containment barrier materials. *Waste Manag.* **2010**, *30*, 2570–2578. [[CrossRef](#)] [[PubMed](#)]
5. Li, S.; Wang, X.M.; Zhang, Q.L. Time-varying characteristic of paste-like super-fineun-classified tailings in long self-flowing transportation. *J. Northeast Univ. Nat. Sci.* **2016**, *37*, 1045.
6. Li, S.; Yu, Q.J.; Wei, J.X. Effect of molecular structure of polycarboxylate water reducers on hydration of cement. *J. Chin. Ceram. Soc.* **2012**, *40*, 613–619.
7. Zhang, B.K. Numerical simulation on property modification and pressure-regulated transportation of filling slurry with full tailings. *Min. Res. Dev.* **2022**, *42*, 116–119.
8. Yang, L.H.; Li, J.C.; Jiao, H.Z.; Wu, A.; Yin, S. Research on the Homogenization Evaluation of Cemented Paste Backfill in the Preparation Process Based on Image Texture Features. *Minerals* **2022**, *12*, 1622. [[CrossRef](#)]
9. Li, C.P.; Yan, B.H.; Hou, H.Z.; Li, R.; Li, X. Rheological behavior of solid liquid conversion stage of unclassified tailings backfill paste. *Chin. J. Nonferrous Met* **2020**, *30*, 1209.
10. Yang, L.H.; Gao, Y.; Yin, S.H.; Jiao, H.Z.; Chen, X.M.; Wang, H.J.; Kou, Y.P. Meso-structure evolution of cemented paste backfill during mixing process based on PVM. *J. China Coal Soc.* **2023**, 1–15. Available online: <https://kns.cnki.net/kcms/detail/11.2190.TD.20220720.1444.006.html> (accessed on 3 August 2023).
11. Trulsson, M.; DeGiuli, E.; Wyart, M. Effect of friction on dense suspension flows of hard particles. *Phys. Rev. E* **2017**, *95*, 012605. [[CrossRef](#)] [[PubMed](#)]
12. Wei, X.F.; Li, W.; Fan, X.Q.; Zhu, M.H. MoS₂-functionalized attapulgite hybrid toward high-performance thickener of lubricating grease. *Tribol. Int.* **2023**, *179*, 108135. [[CrossRef](#)]
13. Xue, Z.L.; Zhang, Y.Z.; Bao, Y.H.; Liu, Z.Y.; Li, Y. Study on rheological property of unclassified-tailing slurry considering the temperature effect. *Met. Mine* **2016**, *10*, 35.
14. Zhang, L.; Lu, Y.Q.; Yu, Y.X.; Li, Q.; Qian, J.Y.; He, X.L. Effect of hydroxypropyl methylcellulose molecular weight on supramolecular structures and properties of HPMC/sodium citrate photophobic films. *Int. J. Biol. Macromol.* **2019**, *137*, 1013–1019. [[CrossRef](#)]
15. Zheng, B.K.; Huang, T.L.; Yin, X.Y.; Zhang, S.; Zhang, L.Y. Experimental study on additives for reducing filling slurry density. *Min. Res. Dev.* **2021**, *41*, 53–56.
16. Wang, L.M.; Yin, S.H.; Deng, B.N.; Wu, A.X. Copper sulfides leaching assisted by acidic seawater-based media: Ionic strength and mechanism. *Miner. Eng.* **2022**, *175*, 107286. [[CrossRef](#)]
17. Üzer, E.; Plank, J. Impact of welan gum stabilizer on the dispersing performance of polycarboxylate superplasticizers. *Cem. Concr. Res.* **2016**, *82*, 100–106. [[CrossRef](#)]
18. Ma, B.; Peng, Y.; Tan, H.; Lv, Z.; Deng, X. Effect of Polyacrylic Acid on Rheology of Cement Paste Plasticized by Polycarboxylate Superplasticizer. *Materials* **2018**, *11*, 1081. [[CrossRef](#)]
19. Patural, L.; Marchal, P.; Govin, A.; Grosseau, P.; Ruot, B.; Deves, O. Cellulose ethers influence on water retention and consistency in cement-based mortars. *Cem. Concr. Res.* **2011**, *41*, 46–55. [[CrossRef](#)]
20. Zhang, Y.; Zhao, Q.; Liu, C.; Zhou, M. Properties comparison of mortars with welan gum or cellulose ether. *Constr. Build. Mater.* **2016**, *102*, 648–653. [[CrossRef](#)]
21. Bulichen, D.; Kainz, J.; Plank, J. Working mechanism of methyl hydroxyethyl cellulose (MHEC) as water retention agent. *Cem. Concr. Res.* **2012**, *42*, 953–959. [[CrossRef](#)]
22. Ghio, V.A.; Monteiro, P.J.M.; Demsetz, L.A. The rheology of fresh cement paste containing polysaccharide gums. *Cem. Concr. Res.* **1994**, *24*, 243–249. [[CrossRef](#)]
23. Isik, I.E.; Ozkul, M.H. Utilization of polysaccharides as viscosity modifying agent in self-compacting concrete. *Constr. Build. Mater.* **2014**, *72*, 239–247. [[CrossRef](#)]
24. Chen, Q.X.; Zhou, H.L.; Wang, Y.M.; Wang, D.L.; Zhang, Q.L.; Liu, Y.K. Erosion wear at the bend of pipe during tailings slurry transportation: Numerical study considering inlet velocity, particle size and bend angle. *Int. J. Miner. Metall. Mater.* **2023**, *30*, 1608–1620. [[CrossRef](#)]
25. Wang, J.X.; Xing, M.H.; Yang, X.L.; Jiao, H.Z.; Chen, F.B.; Yang, L.H.; Yu, J.X.; Fu, Y. Review on the Influence and Control of Sulfur-Containing Tailings on the Strength of Cemented Backfill in Metal Mines. *Buildings* **2023**, *13*, 51. [[CrossRef](#)]
26. Chen, Y.L.; Zhang, Y.M.; Chen, T.J.; Zhao, Y.L.; Bao, S.X. Preparation of eco-friendly construction bricks from hematite tailings. *Constr. Build. Mater.* **2011**, *25*, 2107–2111. [[CrossRef](#)]
27. Yang, L.H.; Li, J.C.; Liu, H.B.; Jiao, H.Z.; Yin, S.H.; Chen, X.M.; Yang, Y. A systematic review of mixing technology for recycling waste tailings as cemented paste backfill in mines of China. *Int. J. Miner. Metall. Mater.* **2023**, *30*, 1430–1443. [[CrossRef](#)]
28. Gu, X.W.; Wang, S.Y.; Liu, J.P.; Wang, H.; Xu, X.C.; Wang, Q.; Zhu, Z.G. Effect of hydroxypropyl methyl cellulose (HPMC) as foam stabilizer on the workability and pore structure of iron tailings sand autoclaved aerated concrete. *Constr. Build. Mater.* **2023**, *376*, 130979. [[CrossRef](#)]
29. Brunchi, C.E.; Morariu, S.; Iftime, M.M.; Stoica, I. Xanthan gum in solution and solid-like state: Effect of temperature and polymer concentration. *J. Mol. Liq.* **2023**, *387*, 122600. [[CrossRef](#)]
30. Wu, A.X.; Ai, C.M.; Wang, Y.M.; Yang, X.X.; Zhou, F.L. Test and mechanism analysis on improving rheological property of paste with pumping agent. *J. Cent. South Univ.* **2016**, *471*, 1513–1529.

31. Zhaidarbek, B.; Tleubek, A.; Berdibek, G.; Wang, Y.W. Analytical predictions of concrete pumping: Extending the Khatib–Khayat model to Herschel–Bulkley and modified Bingham fluids. *Cem. Concr. Res.* **2023**, *163*, 107035. [[CrossRef](#)]
32. Daneshfar, R.; Ashoori, S.; Soulgani, B.S. Interaction of electrolyzed nanomaterials with sandstone and carbonate rock: Experimental study and DLVO theory approach. *Geoenergy Sci. Eng.* **2023**, 212218. [[CrossRef](#)]

Disclaimer/Publisher’s Note: The statements, opinions and data contained in all publications are solely those of the individual author(s) and contributor(s) and not of MDPI and/or the editor(s). MDPI and/or the editor(s) disclaim responsibility for any injury to people or property resulting from any ideas, methods, instructions or products referred to in the content.